Conversion of Core Oxos to Water Molecules by $4e^-/4H^+$ Reductive Dehydration of the $Mn_4O_2^{6+}$ Core in the Manganese−Oxo Cubane Complex $Mn_4O_4(Ph_2PO_2)_6$: A Partial Model for Photosynthetic Water Binding and Activation

Wolfgang F. Ruettinger and G. Charles Dismukes*

Chemistry Department, Hoyt Laboratory, Princeton University, Princeton, New Jersey 08544

Received September 24, 1999

Reaction of the $Mn_4O_4^{6+}$ "cubane" core complex, $Mn_4O_4L_6$ (**1**) (L = diphenylphosphinate, $Ph_2PO_2^-$), with a hydrogen atom donor, phenothiazine (pzH), forms the dehydrated cluster $Mn_4O_2L_6$ (**2**), which has lost two μ-oxo bridges by reduction to water (H_2O). The formation of **2** was established by electrospray mass spectrometry, whereas FTIR spectroscopy confirmed the release of water molecules into solution during the reduction of **1**. UV−vis and EPR spectroscopies established the stoichiometry and chemical form of the pzH product by showing the production of 4 equiv of the neutral pz$^{\cdot}$ radical. By contrast, the irreversible decomposition of **1** to individual Mn(II) ions occurs if the reduction is performed using electrons provided by various proton-lacking reductants, such as cobaltocene or electrochemical reduction. Thus, cubane **1** undergoes coupled four-electron/four-proton reduction with the release of two water molecules, a reaction formally analogous to the reverse sequence of the steps that occur during photosynthetic water oxidation leading to O_2 evolution. ^{1}H NMR of solutions of **2** reveal that all six of the phosphinate ligands exhibit paramagnetic broadening, due to coordination to Mn ions, and are magnetically equivalent. A symmetrical core structure is thus indicated. We hypothesize that this structure is produced by the dynamic averaging of phosphinato ligand coordination or exchange of μ-oxos between vacant μ-oxo sites. The paramagnetic ^{1}H NMR of water molecules in solution shows that they are able to freely exchange with water molecules that are bound to the Mn ion(s) in **2**, and this exchange can be inhibited by the addition of coordinating anions, such as chloride. Thus, **2** possesses open or labile coordination sites for water and anions, in contrast to solutions of **1**, which reveal no evidence for water coordination. Complex **2** exhibits greater paramagnetism than that of **1**, as seen by ^{1}H NMR, and it possesses a broad (440 G wide) EPR absorption, centered at $g = 2$, that follows a Curie−Weiss temperature dependence (10−40 K) and is visible only at low temperatures, compared to EPR-silent **1**. Its comparison to a spin-integration standard reveals that **2** contains 2 equiv of Mn(II), which is in agreement with the formal oxidation state of 2Mn(II)2Mn(III) that was derived from the titration. The EPR and NMR data for **2** are consistent with a loss of two of the intermanganese spin-exchange coupling pathways, versus **1**, which results in two "wingtip" Mn(II) $S = 5/2$ spins that are essentially magnetically uncoupled from the diamagnetic Mn_2O_2 base. Bond-enthalpy data, which show that O_2 evolution via the reaction $\mathbf{1} \rightarrow \mathbf{2} + O_2$, is strongly favored thermodynamically but is not observed in the ground state due to an activation barrier, are included. This activation barrier is hypothesized to arise, in part, from the constraining effect of the facially bridging phosphinate ligands.

Introduction

Photosynthetic oxygen evolution by water oxidation is catalyzed by a unique metalloenzyme that contains the same invariant inorganic core in all plants, comprising a spin-coupled tetramanganese cluster, a Ca^{2+} ion, and an unknown number of Cl^- ions.[1−4] The structure of the tetrameric Mn core is incompletely established but is believed to possess a pair of oxo-bridged Mn_2 cores with Mn−Mn separations of 2.7 and 3.3 Å, assigned using Mn EXAFS.[5,6] The water-oxidizing complex (WOC) is an integral part of the Photosystem II reaction center protein complex (PSII) and includes an essential tyrosyl radical cofactor that mediates sequential one-electron transfer steps to produce five oxidation states, designated S_0, S_1, ...S_4.

Functional modeling of the WOC, by synthesis of tetranuclear Mn complexes that catalyze water oxidation, has not been achieved.[7−15] Nor have stable tetramanganese complexes that

(1) Ananyev, G. M.; Dismukes, G. C. *Biochemistry* **1997**, *36*, 11342−11350.
(2) Debus, R. J. *Biochim. Biophys. Acta* **1992**, *1102*, 269−352.
(3) Zaltsman, L.; Ananyev, G.; Bruntrager, E.; Dismukes, G. C. *Biochemistry* **1997**, *36*, 8914−8922.
(4) Yachandra, V. K.; Sauer, K.; Klein, M. P. *Chem. Rev.* **1996**, *96*, 2927−2950.
(5) Yachandra, V. K.; DeRose, V. J.; Latimer, M. J.; Mukerji, I.; Sauer, K.; Klein, M. P. *Science* **1993**, *260*, 675−679.
(6) Penner-Hahn, J. E.; Riggs-Gelasco, P. J.; Yu, E.; DeMarois, P.; Yocum, C. F. In *Proceedings of the Xth International Photosynthesis Conference*; Mathis, P., Ed.; Kluwer Academic Press: Montpellier, France, 1995; Vol. 2, pp 241−246.
(7) Wieghardt, K. *Angew. Chem., Int. Ed. Engl.* **1989**, *28*, 1153−1172.
(8) Vincent, J. B.; Christou, G. *Adv. Inorg. Chem.* **1989**, *33*, 197−257.
(9) Aromi, G.; Wemple, M. W.; Aubin, S. J.; Folting, K.; Hendrickson, D. N.; Christou, G. *J. Am. Chem. Soc.* **1998**, *120*, 5850−5851.
(10) Armstrong, W., Pecoraro, V. L., Ed.; VCH: New York, 1992; pp 261−286.
(11) Dube, C. E.; Wright, D. W.; Pal, S.; Bonitatebus, P. J., Jr.; Armstrong, W. H. *J. Am. Chem. Soc.* **1998**, *120*, 3704−3716.
(12) Gorun, S. M.; Stibrany, R. T.; Lillo, A. *Inorg. Chem.* **1998**, *37*, 836−837.
(13) Manchandra, R.; Brudvig, G. W.; Crabtree, R. H. *Coord. Chem. Rev.* **1995**, *144*, 1−38.

10.1021/ic9911421 CCC: $19.00
Published on Web 02/10/2000

exhibit four-electron redox chemistry of any type, a hallmark of the WOC, yet been characterized . To date, only two structurally characterized Mn compounds are known to catalyze water oxidation.[16] One of these, Mn_6−silesquioxane, is a hexanuclear cluster that works as a heterogeneous catalyst with low activity and stability.[17] The other is a covalently linked perfluorinated-dimangano−porphyrin complex that is active for a few turnovers.[18] Recently, the production of O_2 from peroxomono sulfate (SO_5^{2-}) or hypochlorite (ClO^-) using a Mn dimer as the catalyst was also reported.[19,20]

An earlier proposal for the structural rearrangements of the WOC conjectured a $Mn_4O_4^{n+}$ to $Mn_4O_2^{n+}$ (cubane-to-butterfly) core conversion during the oxygen-evolving step.[21] Data from X-ray absorption studies[5,6] have excluded a symmetrical cubane Mn_4O_4 or butterfly Mn_4O_2 core for the S_1-S_3 oxidation states of the WOC, whereas EPR studies have eliminated the symmetrical cubane core.[22−26] However, distorted cuboidal structures ($Mn_4O_2X_2$, C_{2v} or D_{2d} symmetries) were shown to provide accurate simulations of the S_2 EPR signals.[22] Herein, we demonstrate the first $Mn_4O_4^{n+}$ to $Mn_4O_2^{n+}$ core conversion by reductive dehydration of μ-oxos to form two water molecules.

Materials and Methods

All of the chemicals were reagent grade and used as received. Dichloromethane and acetonitrile were HPLC grade (<0.002% H_2O). The CH_2Cl_2 solvent for the FTIR studies was distilled over CaH_2 and stored over a 3 Å molecular sieve under Ar. $Mn_4O_4(Ph_2PO_2)_6$ (**1**) was synthesized as described[27] and recrystallized from dichloromethane.

The NMR spectra were recorded on a General Electric/Tecmag 300 MHz spectrometer. The IR spectra were recorded on a NICOLET FTIR spectrometer using either KBr pellets or a liquid FTIR cell with KBr windows and a 0.5 mm path length. The EPR spectra were recorded on a Bruker ESP300 spectrometer equipped with an Oxford 900 cryostat and either a Bruker TE102 or a Bruker ER4116DM9601 dual mode X-band EPR cavity for low-temperature work. The measurement parameters are as indicated in the figure captions. The UV−vis spectra were recorded on an HP8452 spectrophotometer using a 10 mm quartz cuvette. Titrations of **1**, with phenothiazine (pzH), were performed in dichlormethane at concentrations of 0.05 and 0.2 mM of **1** and stock solutions of 5 or 50 mM of pzH, respectively. Electrospray ionization (ESI) mass spectra were recorded on a Hewlett-Packard HP5989B spectrometer using CH_3CN as the eluent with a capillary voltage of 25 V.

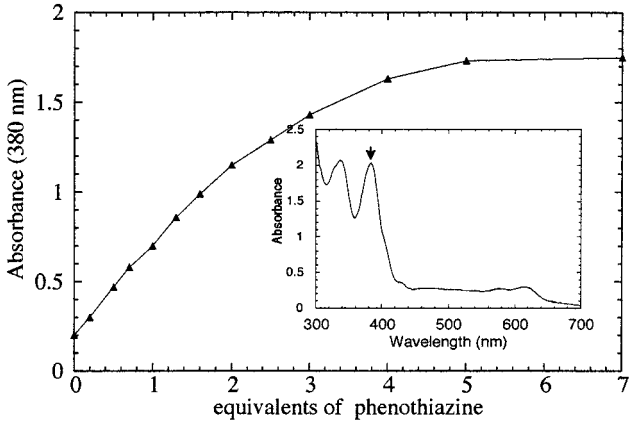

Figure 1. Absorption change at 380 nm (λ_{max} of the neutral pz$^{\cdot}$ radical) during the titration of 0.05 mM of **1** with phenothiazine (PZH). The inset shows the UV−vis spectrum of the reaction mixture containing 0.2 mM of **1** and 2 equiv of pzH.

Results

On the basis of crystal structure and ^{1}H NMR data, $Mn_4O_4L_6$ (**1**) (L = diphenylphosphinate) was found to have an approximately symmetrical cubane core with formal Mn oxidation states 2III, 2IV.[27] We explored the possibilities of a one-electron reduction of **1** by reaction with cobaltocene ($CoCp_2$) and an electrochemical reduction on Pt and glassy carbon electrodes. However, these reactions lead to multielectron reduction, coupled with the irreversible decomposition of the cubane core and the release of free Mn(II), as seen by EPR spectroscopy. No intermediate reduced species could be detected, even at substoichiometric amounts of reductant, indicating the instability of the one-electron reduced cluster, presumably due to fast bimolecular disproportionation after the initial one-electron reduction.

The disproportionation reaction was avoided by performing the reduction with the hydrogen atom donor phenothiazine (pzH)[28−30] (Figure 1). The titration of **1** with pzH in CH_2Cl_2 solution was found to reach an end point after the addition of 4 equiv and produced the neutral pz$^{\cdot}$ radical, characterized by UV−vis spectrophotometry (Figure 1) and room-temperature EPR spectroscopy (Figure 2A). This assignment was confirmed by a simulation of the EPR signal for the pz$^{\cdot}$ radical, using the published hyperfine constants. It was further established by the protonation of the radical with acid to form the pzH$^+$ cation radical (Figure 2B).[30] An unusually long lifetime of the pz$^{\cdot}$ radical was observed in the reaction mixtures (no decay was observed within minutes), suggesting the reversible formation of a weak complex between the reduced cluster **2** and pz$^{\cdot}$.

Further evidence for weak-complex formation between **2** and pz$^{\cdot}$ came from the fact that the EPR signal of the radical could not be saturated (200 mW microwave power) even at 10 K, which is in contrast to the normal beavior of free radicals, in general. Hence, the radical exhibits unusually rapid spin relaxation. In addition, no clear end point in the titration of **1** with pzH is seen by EPR spectroscopy. The area of the pz$^{\cdot}$ radical signal continues to increase by ∼60% between 4 and 10 equiv of pzH, whereas the UV−vis (of the pz$^{\cdot}$ radical) and the NMR (of pzH) spectroscopies both reach an end point at 4 equiv (95% maximum). The free pzH in the NMR spectra appear only after more than 4 equiv have been added. The yield of the

(14) Micklitz, W.; Bott, S. G.; Bentsen, J. G.; Lippard, S. J. *J. Am. Chem. Soc.* **1989**, *111*, 372−374.
(15) Darovsky, A.; Kezerashvili, V.; Coppens, P.; Weyermuller, T.; Hummel, H.; K., W. *Inorg. Chem.* **1996**, *35*, 6916−6917.
(16) Rüttinger, W.; Dismukes, G. C. *Chem. Rev.* **1997**, *97*, 1−24.
(17) Kuznetsov, V. L.; Elizarova, G. L.; Matvienko, L. G.; Lantyukova, I. G.; Zhdanov, A.; Shchegolkhina, O. I. *J. Organomet. Chem.* **1994**, *475*, 65−72.
(18) Naruta, Y.; Sasayama, M.; Sasaki, T. *Angew. Chem., Int. Ed. Engl.* **1994**, *33*, 1839−1841.
(19) Limburg, J.; Vrettos, J. S.; Liable-Sands, L. M.; Rheingold, A. L.; Crabtree, R. H.; Brudvig, G. W. *Science* **1999**, *283*, 1524−1528.
(20) Limburg, J.; Brudvig, G. W.; Crabtree, R. H. *J. Am. Chem. Soc.* **1997**, *119*, 2761−2762.
(21) Vincent, J. B.; Christou, G. *Inorg. Chim. Acta* **1987**, *136*, L41−43.
(22) Zheng, M.; Dismukes, G. C. *Inorg. Chem.* **1996**, *35*, 3307−3319.
(23) Bonvoisin, J.; Blondin, G.; Girerd, J. J.; Zimmermann, J. L. *Biophys. J.* **1992**, *61*, 1076−1086.
(24) Dismukes, G. C. In *Mixed Valency Systems: Applications in Chemistry, Physics and Biology*; Prassides, K., Ed.; Kluwer Acad. Publ.: Boston, 1991; Vol. 343, pp 137−154.
(25) Dismukes, G. C.; Tang, X.-S.; Khangulov, S. V.; Sivaraja, M.; Pessiki, P.; Zheng, M. In *Research in Photosynthesis*; Kluwer Academic Publ.: Dordrecht, 1992; Vol. 2, pp 257−264.
(26) Kusunoki, M. *Chem. Phys. Lett.* **1992**, *197*, 108−116.
(27) Ruettinger, W.; Campana, C.; Dismukes, G. C. *J. Am. Chem. Soc.* **1997**, *119*, 6670−6671.
(28) Billon, J.-P. *Bull. Soc. Chim. Fr.* **1961**, 1923−1929.
(29) Billon, J.-P. *Ann. Chim. (France)* **1962**, *7*, 190−196.
(30) Gilbert, B. C.; Hanson, P.; Norman, R. O. C.; Sutcliffe, B. T. *Chem. Commun.* **1966**, *6*, 161−164.

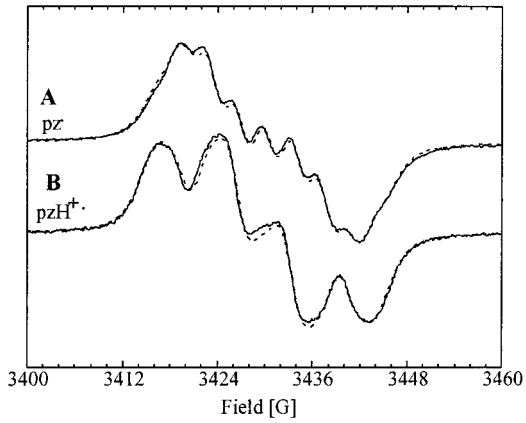

Figure 2. Room-temperature EPR spectra of (A) a reaction mixture containing 0.2 mM of **1** and 4 equiv of pzH in CH_2Cl_2, showing the pz˙ (neutral) radical, and (B) the same solution after the addition of CF_3COOH, showing the conversion to the $pzH^{\bullet+}$ (cation) radical. Measurement conditions: 9.46 GHz; mod freq = 100 kHz; mod amp = 0.1 G; time const = 10 ms; 4 scans; simulations: using published[30] hyperfine parameters (for $pzH^{\bullet+}$ [G]: $a_N = 6.52$; $a_{N-H} = 7.36$; a_H = 1.23 ($H_{1,9}$), 0.46 ($H_{2,4,6,8}$), 2.58 ($H_{3,7}$); for pz˙ [G]: $a_N = 7.06$; a_H = 2.68 ($H_{1,9}$), 1.00 ($H_{2,8}$), 3.64 ($H_{3,7}$), 0.73 ($H_{4,6}$)) and 2.0 G line width.

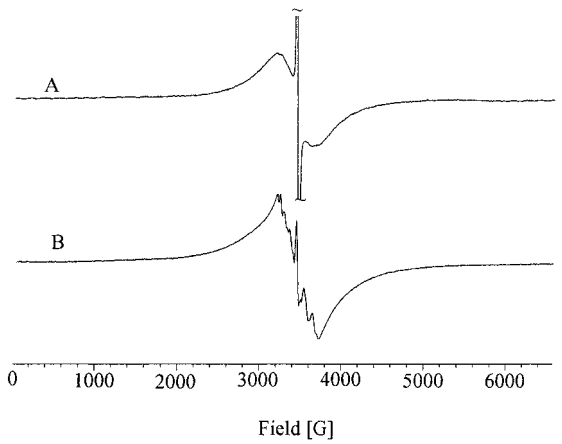

Figure 3. (A) EPR spectrum of **2** + pz˙ after complete reduction of 0.3 mM of **1** with 5 equiv of pzH in CH_2Cl_2, T = 7.5 K; **(B)** EPR spectrum of **2** after complete reduction of **1** in the presence of 5 mM of NEt_4Cl, T = 14 K; Both spectra recorded at 9.66 GHz, power = 20 mW, mod freq = 100 kHz, mod amp = 10 G, time const = 20 ms.

pz˙ radical EPR signal at room temperature was found to be only ~60% of the expected value, between 1 and 3 equiv of pzH. The addition of excess pzH (10 equiv) increased the amount of the narrow pz˙ radical to ~85% of the 4 equiv that were expected. This behavior indicates the formation of a weak complex between the pz˙ radical and the reduced **1** that can be dissociated by excess pzH, leading to an increase in the radical signal seen by EPR. Further support for this complex formation was found by rapid-mixing stopped-flow UV−vis measurements (M. Maneiro, unpublished results).

The parent cluster **1** is EPR silent using conventional X-band microwave excitation (B_0 perpendicular to B_1). Figure 3A illustrates the low-temperature EPR signal for the reduced cluster **2** that forms by the addition of 4 equiv of pzH to a solution of **1**. The signal is approximately 440 G wide, is centered near g = 2, and lacks resolved hyperfine couplings. No free Mn^{II} was observed by EPR spectroscopy, even after the addition of excess pzH (up to 10 equiv). Thus, a stable end point is reached. The total signal area of a sample containing 0.28 mM of **2**, measured at a temperature of 17 K, was within 10% of the area from a Mn(II) spin-concentration standard at 0.5 mM ($Mn(OAc)_2$) that was measured at the same temperature (the 50 G wide pz˙ radical signal contributes less than 2% to the total integral). This concentration fits well with the predicted presence of two uncoupled Mn(II) spins per molecule of **2**. No intermediates were observed in the reduction using cryo-EPR spectroscopy with substoichiometric amounts of the reductant. The broad EPR signal can only be detected at temperatures below ~110 K, and the EPR transition could not be power saturated, even at 7 K. This behavior indicates that the signal is attributable to a fast relaxing spin system, as might be expected from a spin-coupled Mn_4(2II, 2III) cluster with a paramagnetic ground state. The cluster EPR signal obeys a Curie−Weiss temperature dependence below 40 K, with a plot of the intensity versus $1/T$ behaving linearly and a nonzero intercept with the Weiss constant = 7−9 K (see Figure S6 in the Supporting Information). The addition of 5 mM of NEt_4Cl to the reaction mixture leads to the conversion of the EPR signal to one of similar width and integral area, but also shows resolved ^{55}Mn hyperfine splittings in the 40−106 G range (Figure 3B). In addition, the decay of the pz˙ radical becomes much faster (minutes). This behavior suggests that Cl^- ions bind to the cluster and either slow the relaxation time or reduce the inhomogeneous broadening, leading to resolution of the Mn hyperfine structure. The binding of Cl^- suppresses the interaction of **2** with the pz˙ radical, thereby increasing the yield of the pz˙ radical signal. The magnetic interaction between the pz˙ radical and **2** must be weak, in comparison with the broad, inhomogeneous line width of **2** (<1200 MHz). Hence, the integral of **2**, observed in frozen solutions, does not reflect the appreciable loss of spin due to coupling to the pz˙ radicals, in contrast to the narrow (room temperature) spectrum of the pz˙ radcial, which is in rapid chemical exchange between bound and free pz˙ radicals.

The EPR signal properties for **2** are not those expected for free Mn(II) ions or free Mn(III) ions; Mn(III) ions typically have very large zero-field splittings,[31] whereas the spin relaxation rate of free Mn(II) ions is much slower than in **2**, as is evident from the unobserved power saturation for **2**. However, the spin quantitation for **2** suggests that there is the equivalent of two Mn(II) spins present. Compound **2** is predicted to have formal Mn oxidation states of 2II, 2III, based on the observed stoichiometry of four pz˙ radicals formed, which would be consistent with the spin integration. There are 10 electronic states predicted for a coupled cluster in the 2II, 2III oxidation state corresponding to states with spin S = 0, 1, ..., 9. For example, the carboxylate-bridged complexes, $Mn_4O_2(RCO_2)_6$ containing the slightly bent $Mn_4O_2^{6+}$ butterfly core, were found to have an intermediate-spin S = 2 ground state with several low-lying spin states.[32] This result indicates the presence of both antiferromagnetic and ferromagnetic exchange interactions (J) between Mn pairs. A self-consistent interpretation of the EPR-spectral and -intensity data for **2** is that it is composed of two S = 5/2 Mn(II) ions that are uncoupled or weakly coupled ($J \ll kT$). The bridging unit (Mn_2O_2) is a pair of Mn(III) ions that are strongly antiferromagnetically coupled ($J' \gg kT$) and, therefore, are EPR invisible, in much the same way that a closed-shell carboxylate bridge is EPR invisible. Such a ground-state configuration would be expected to produce an EPR signal resembling free Mn(II) ions (at temperatures $kT > J$) with a simple uncoupled "six line" ^{55}Mn hyperfine spectrum and a spin

(31) Barra, A.-L.; Gatteschi, D.; Sessoli, R.; Abbati, G. L.; Cornia, A.; Fabretti, A. C.; Uytterhoeven, M. G. *Angew. Chem., Int. Ed. Engl.* **1997**, *36*, 2329−2331.
(32) Vincent, J. B.; Christmas, C.; Chang, H.-R.; Li, Q.; Boyd, P. D. W.; Huffman, J. C.; Hendrickson, D. N.; Christou, G. *J. Am. Chem. Soc.* **1989**, *111*, 2086−2097.

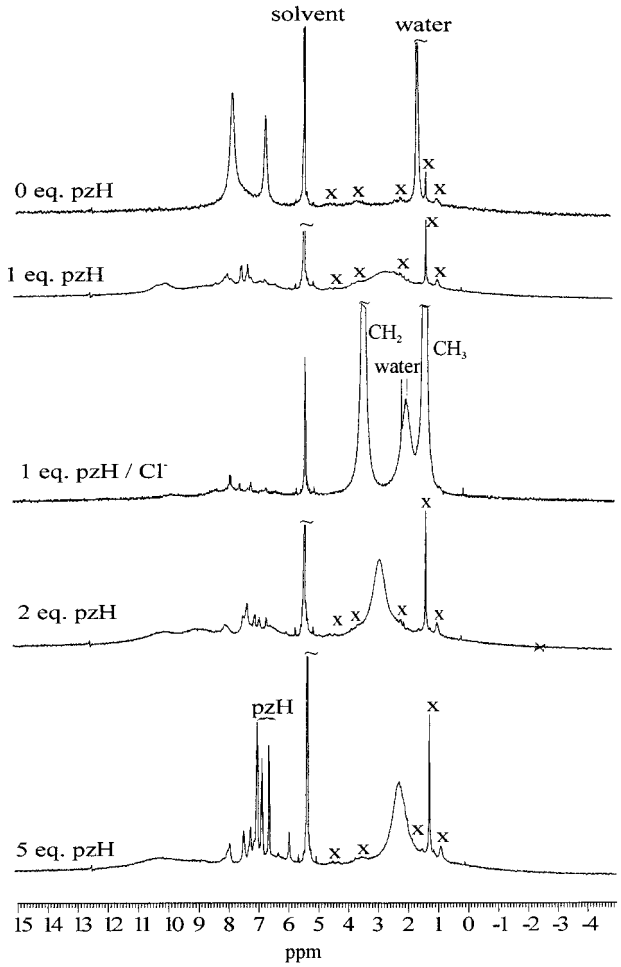

Figure 4. NMR spectra (300 MHz) of (A) 0.32 mM of **1** in CD_2Cl_2 (B) after addition of ~1 equiv of pzH (5 mM in CD_2Cl_2) (C) after addition of ~1 equiv of pzH in the presence of 5 mM of NEt_4Cl (D) after addition of ~2 equiv of pzH (E) after addition of 5 equiv of pzH; solvent impurities are marked with X.

concentration equal to two Mn(II) ions but with increased relaxation owing to transient population of excited spin states.

^{1}H NMR spectroscopy was used to identify the fate of the $Ph_2PO_2^-$ ligands upon reduction **(**Figure 4). The 60 phenyl protons in **1** have been quantitatively accounted for by the three paramagnetically broadened peaks at 6.63 ppm (para), 7.75 ppm (meta), and 7.4 ppm (ortho), which also establishes the equivalence of all six diphenylphosphinate ligands in **1**.[27] These resonances disappear after reduction with 1 equiv of pzH, together with formation of a lower symmetry intermediate(s) with new resonances at 10.25, 9.93, 8.29, 7.98, 7.89, 7.72, 7.42, 7.21, 7.10, 6.78, 6.65, 6.28, and 5.2 ppm. Scans over a wider range of +40 to −20 ppm failed to reveal other resonances. Importantly, the water proton resonance at 1.5 ppm, which is present in the solvent, disappears completely after the addition of 1 equiv of pzH to the solution of **1** in methylene chloride. The water concentration, relative to the concentration of **1**, is equal to 15:1 on a per mole basis. This loss of signal indicates that a new interaction occurs between water and the initial product(s) of this reaction, which eliminates the free-water signal. The new broad resonance, which appears after the addition of 1 equiv of pzH centered at 2.4 ppm, apparently represents these water molecules. The shift indicates an enhanced paramagnetism in the reduced cluster, whereas the increased broadening indicates a faster spin-relaxation rate for the water spins. Both of these effects are expected if the

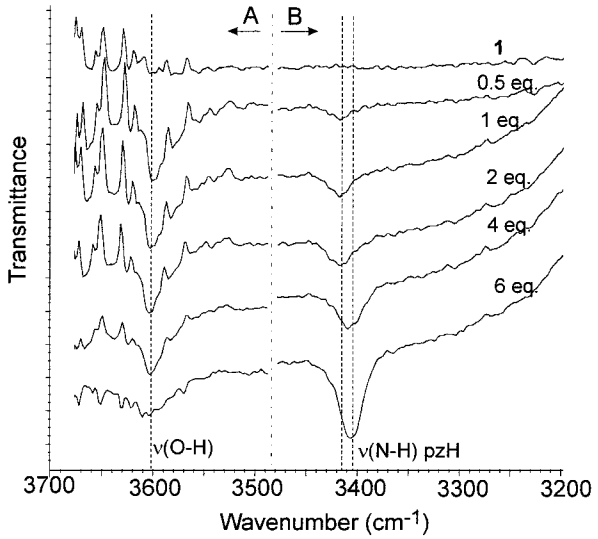

Figure 5. FTIR spectra of reaction mixtures containing 1 mL of **1** (0.33 mM in CH_2Cl_2) and pzH (10 mM in CH_2Cl_2; 33 μL per equiv) in solution. The left part (A) was corrected for contributions from water contained in the pzH solution (<10% of the peak at 3600 cm^{-1} at 1 equiv of pzH; see Supporting Information) by subtracting the appropriate pzH solution reference spectrum. The right part (B) is not corrected for pzH contributions. Conditions: corrected for KBr windows + solvent as background spectrum, 256 scans.

reduction of **1** produces Mn(II) ions in **2** and these sites can bind water molecules from solution. We cannot exclude the possibility that this peak may include some phenyl protons from the phosphinate ligands that bind to the reduced intermediate because integration was unreliable, due to its extremely broad line width. The NMR spectrum changes further with additional pzH (Figure 4). At 2 equiv of pzH, the (water) peak moves to 2.7 ppm and sharpens, whereas at 5 equiv of pzH, it moves to 2.2 ppm and remains there with addition of excess pzH. The addition of NEt_4Cl to the solution in ~20× excess (5 mM) leads to a significantly sharper resonance for the water protons, indicating that Cl^- may bind to the cluster and displace water as a ligand. Other peaks in the spectrum also reach an end point at 4 equiv of pzH, corresponding to the final product **2**, which exhibits broad peaks centered at 10.2, 8.8, and 6.3−7 ppm. These peaks are assigned to the ring phenyl protons in the final product **2**. These peaks exhibit greater line broadening than that of **1**, indicative of the enhanced paramagnetism that is consistent with weaker electronic-exchange couplings. In addition, sharper features are seen at 7.9, 7.4, 7.2, and 5.9 ppm, corresponding to a minority species. The former three of these sharp features arise after the addition of 1 equiv of pzH and do not increase proportionally and may, therefore, not be attributable to **2**. Three resonances due to unreacted pzH can be seen at 6.98, 6.83, and 6.58 ppm after more than 4 equiv of pzH are added.

Solution FTIR spectroscopy (Figure 5) was used to probe the formation of water upon the reduction of **1** with pzH and to characterize **2** in more detail. During the titration of **1** it was found that the NH vibration of free pzH (υ = 3405 cm^{-1}) appeared only after more than 4 equiv of pzH were added to **1**, in agreement with the UV−vis and NMR spectral titrations. In addition, two new IR bands were observed at 3415 and 3600 cm^{-1}. The 3415 cm^{-1} peak was detectable after the addition of 0.5 equiv of pzH and reached a maximum between 1 and 2 equiv of pzH. The peak shifted between 2 and 4 equiv of pzH to the position of free pzH (3405 cm^{-1}) and was barely visible with excess pzH. The 3600 cm^{-1} band increases peak intensity slightly, together with broadening from 0.5 to 4 equiv of pzH.

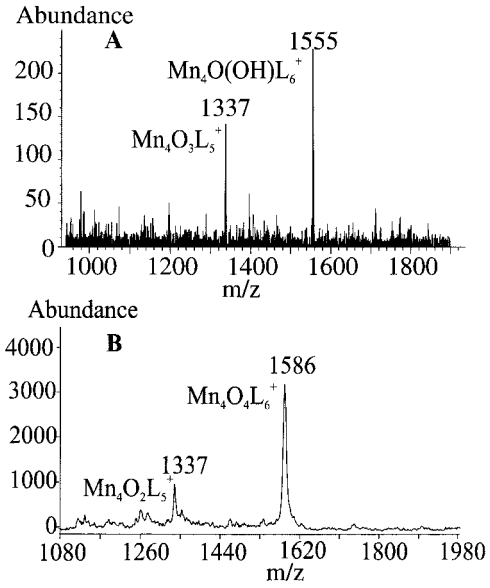

Figure 6. (A) Electrospray ionization mass spectrum of a solution **1** (60 μM) and 4 equiv of pzH in CH_2Cl_2/CH_3CN (1/4). Average of 1.5 to 4.2 min spectral accumulation with CH_3CN as the eluent. (B) Laser desorption ionization-time-of -flight mass spectrum of **1** (no matrix; positive ion) recorded on a Hewlett-Packard G2025A mass spectrometer using a N_2 laser; $\lambda = 337$ nm).

Neither the 3415 nor the 3600 cm^{-1} bands are significantly present in controls containing only **1** or pzH. The 3600 cm^{-1} band can be positively assigned to a water-O−H mode on the basis of a control sample containing 5mM of water in dry CH_2Cl_2 solvent, which exhibits an identical IR band at 3600 cm^{-1} (see Figure S9 in the Supporting Information).

Electrospray ionization mass spectrometry (ESIMS) has proven to be a powerful method for the detection of oxo-bridged Mn complexes.[33] Positive-ion ESIMS of the pzH reduction product **2 (**Figure 6A) shows the appearance of only two peaks above $m/z = 920$. The dominant fragment peak (m/z 1555) arises from the species $(\mathbf{1} - m/z\ 32)^+$, which is consistent with the removal of two bridging oxo ions as water molecules from the cubane core (Scheme 1). The second (less abundant) fragment peak (m/z 1337) can be assigned to the species $(\mathbf{1} - m/z\ 217 - m/z\ 32)^+$, in which one $Ph_2PO_2^-$ ligand (mass 217) and two O atoms (as water molecules) are removed. The major species at m/z 1555 can be assigned to $\mathbf{2}H^+$, formed by the protonation of **2** under the ESI ionization conditions, whereas the minor species, m/z 1337, corresponds to loss of one diphenylphosphinate anion from **2** (detection of $[\mathbf{2} - m/z\ 217]^+$). No signals were observed at higher masses (up to m/z 2000). Unlike **2**, the parent cubane **1** is insoluble in polar solvents and, therefore, could not be examined by ESIMS. The parent ion peak for $\mathbf{1}H^+$ has a predicted m/z of 1587. The parent cation species $\mathbf{1}^+$ is observable using laser desorption−ionization mass spectrometry at m/z 1586, as shown in Figure 6B.[35] The LDI-TOF (laser desorption ionization-time of flight)data in Figure 6B show that laser photolysis of **1** *in the gas phase* also produces only one other species at m/z of 1337, corresponding to the exact mass of $Mn_4O_2L_5$.

Scheme 1

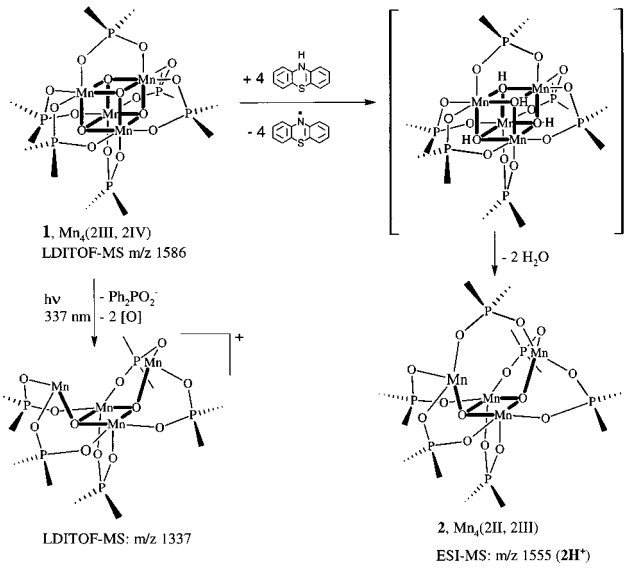

So far, attempts to isolate **2** as a pure solid have failed. Solutions of **2** in CH_2Cl_2 solvent were observed to be unstable over the course of 1 day. UV−vis and EPR analyses of the material isolated from the reaction mixtures after solvent evaporation show that further bleaching and release of Mn(II) occur. Mass (LDI-TOF) and infrared spectral data of the recovered gray solid indicate that the $Mn_4O_2^{6+}$ core is no longer present, but instead, a Mn(II)-diphenylphosphinate polymer is isolated whose IR-spectrum is closely analogous to that of polymeric $[Mn(II)(py)_2(Ph_2PO_2)]_\infty$, a homogeneous white solid that was obtained independently.[34] The cause of the instability of solutions of **2** may be attributable to the availability of open or labile coordination sites on the Mn ions, as seen by NMR. The addition of coordinating anions, such as chloride and bromide, was found to increase the stability of solutions of **2**, consistent with the blocking of open coordination sites for ligand rearrangement that must occur for polymerization.

Discussion

In Scheme 1, we summarize the solution chemistry between pzH and **1**, which can account for the formation of the reduced cluster and propose a possible structure for **2**. This chemistry leads to the formation of neutral rather than charged products, which appears to be influenced by the nonpolar and poor hydrogen-bonding character of the methylene chloride solvent. The reaction takes a different course in more polar solvents or if basic molecules, such as tertiary amines, are present in solution. The initial low-symmetry hydrogenated intermediate (seen by NMR and FTIR) that forms upon the substoichiometric reduction of **1** with pzH is readily reduced further in excess pzH to form a single dominant product, perhaps initially via the fully hydrogenated species, $\mathbf{1}H_4$. This unobserved intermediate is unstable to dehydration and loses two water molecules to form the observed product $[Mn_4O_2L_6]$ (**2**) as seen in mass spectra **(**ESIMS; Figure 6A). Further support for a deoxygenation reaction comes from the LDI-TOF data in Figure 6B, which shows that laser photolysis of **1** *in the gas phase* also produces the species at an m/z of 1337, corresponding to additional loss of one ligand forming $Mn_4O_2L_5$ (Scheme 1). Compound **2** is a neutral species possessing a formal Mn oxidation state of (2II, 2III), based on the stoichiometry of the reaction with pzH. Loss

(33) Andersen, U. N.; McKenzie, C. J.; Bojesen, G. *Inorg. Chem.* **1995**, *34*, 1435−1439.

(34) The compound $[Mn_2\mu\text{-}(Ph_2PO_2)_2py_2]$ was synthesized by slowly evaporating a solution containing **1** (0.3 mM in CH_2Cl_2) and 50 equiv of Me_3SiN_3 in the presence of 0.1% pyridine; single crystals were isolated from the reaction mixture; a preliminary X-ray structure revealed the presence of the chain polymer $[Mn_2\mu\text{-}(Ph_2PO_2)_2py_2]_\infty$.

(35) Ruettinger, W. F.; Ho, D. M.; Dismukes, G. C. *Inorg. Chem.* **1999**, *38*, 1036−1037.

of water from $\mathbf{1}H_4$ would be compatible with the unusually long, and therefore weak, Mn−O(oxo) bonds in **1**.[27] The bond lengths in **1** are 1.92−1.98 Å, which are ∼0.1−0.2 Å longer than the typical Mn−(μ-O) distances in $Mn^{III,IV}_2(\mu\text{-O})_2$ dimers (1.78−1.84 Å).[13] Also, it is relevant that the reduction of $Mn_2O_2^{3+/4+}$ core complexes also leads to release of a water molecule derived from the μ-oxo bridge and the formation of the deoxygenated Mn_2O^{4+} core.[36−38]

Although the structure of **2** is incompletely established, the NMR and mass spectral analyses indicate a species with all six $Ph_2PO_2^-$ ligands bound. The ESIMS data reveal that one of the $Ph_2PO_2^-$ ligands can be forced to dissociate from **2** in a minority of the clusters during the ESI ionization process in the mass spectrometer. The ^{1}H NMR spectrum of **2** is extremely simple and indicates a very high-symmetry environment for the phosphinate ligands, all of which are magnetically equivalent in solution at room temperature. The static structure for **2**, proposed in Scheme 1, has a lower symmetry with three different phosphinate environments. To reconcile this, we propose the possibility of dynamic averaging due either to rapid intramolecular exchange of phosphinates between these sites or to a novel intramolecular μ-oxo atom exchange mechanism with vacant μ-oxo sites. Hence, we propose in Scheme 1 that **2** may have a deoxygenated cubane core in which all six phosphinate ligands remain chelated to Mn sites across the faces of the cube and two oxos are removed as water molecules. Although this structural proposal for **2** is consistent with all of our data, other structures, differing in terms of the phosphinate ligand coordination, are possible, because the dynamic averaging process could again simplify the NMR spectrum.

Although the proposed structure for $\mathbf{2}H^+$ *in the gas phase* contains coordinately unsaturated Mn(II) and Mn(III) ions, having four and five donor atoms,[13] respectively, the structure is undoubtedly coordinated in solution by solvent molecules that can be easily displaced. The NMR data show that solution **2** has a higher coordination number with one or possibly both of these sites bound to water (and possibly an acetonitrile solvent). ESIMS data show that **2** has lost two oxo atoms. The number of water molecules produced in the reduction of **1** could not be measured directly by MS or NMR due to instrumental limitations, but water formation was established by FTIR. NMR also revealed that the water molecules present in solutions of **2** experience strong contact shift and paramagnetic broadening, in contrast to the absence of such effects for solutions of **1**. Thus, water binds to the Mn ions in **2** but not to those in **1**, as would be expected if open or labile coordination sites exist on **2**. FTIR spectroscopy shows a loss of intensity for the NH vibration of pzH (3405 cm^{-1}) when **1** is present and 4 or fewer equiv of pzH are added. During the titration with pzH, a narrow, water-OH mode (3600 cm^{-1}) first appears, consistent with the release of water from **1**, and broadens with increasing addition of pzH. The broadening is attributed to a progressively greater interaction of the released water with H-bonding partners formed in the nonpolar solvent as the titration proceeds (water and excess pzH). An unidentified intermediate (3415 cm^{-1}), possibly coordinated Mn−O−H or hydrogen-bonded N−H···O forms at intermediate pzH concentrations during the titration.

Taken together, the NMR and FTIR data indicate that the water formed upon reduction of **1** is undergoing chemical exchange at the paramagnetic center with labile coordination site(s) on Mn ion(s). This binding site(s) on the reduced cluster can be blocked by the addition of coordinating anions, such as chloride, as seen by NMR, and it may also account for the suppression of oligomerization in solution, upon the stripping of the solvent in the presence of chloride or bromide.

Both NMR and EPR spectroscopies reveal that **2** is paramagnetic between 6 and 300 K. The ground state of **2** is EPR-active with principal absorption at $g = 2$ and can exhibit resolved ^{55}Mn hyperfine structure following the addition of coordinating anions. Compound **2** has low-lying spin states that, when thermally populated, lead to rapid spin relaxation and may also be the source of the weak Curie−Weiss temperature dependence of solutions. EPR spin integration indicates that **2** contains the equivalent of two Mn(II) ions. The Mn(III) ions that are predicted to be present, based on the stoichiometry of the reaction with pzH, do not contribute to the EPR intensity, other than to induce dipolar broadening and relaxation. Their proposed absence from the EPR transition probability would require that the intermanganese spin-exchange couplings (*J* values) are weak, that is, less than or equal to the single-ion ZFS (zero field splitting) from Mn(III) ions.[50] The ZFS values can be as large as 5−10 cm^{-1} for Mn(III) complexes (ref 31). So far, all of the data we have collected for **2**, including the stoichiometry, charge neutrality, and EPR, indicate that the proposed oxidation-state assignment of (2II, 2III) is the most likely assignment, but this is not a definitive assignment.

Compound **1**, and its partially hydrogenated intermediates, are able to break the NH bond of pzH ($\Delta H = 82.3$ kcal/mol[39]), which has an enthalpy that is comparable to the OH bond in tyrosine, the endogenous oxidant for the manganese cluster in the WOC (86.5 kcal/mol[40,41]). Thus, the dehydrogenation of pzH by **1** provides a potential example for examining four successive redox steps (H atom transfer steps or coupled H^+/e^- transfer*)* analogous to the proposed models for tyrosyl radical function in the WOC.[41−43] Table 1 provides an estimate for the bond enthalpy of dissociation for two O atoms from cubane **1** to form **2**, eq 4, obtained from a thermodynamic cycle using the gas-phase bond-dissociation enthalpy of the NH-bonds in pzH, eq 1; the gas-phase bond enthalpy of formation for four O−H bonds in two water molecules, eq 2, and the negative free energy of the spontaneous reduction reaction of **1** with pzH, eq 3. From

(36) Dismukes, G. C. In *Bioinorganic Catalysis*; Reedijk, J., Ed.; Marcel-Dekker: Amsterdam, 1992; pp 317−346.
(37) Sheats, J. E.; Czernuszewicz, R.; Dismukes, G. C.; Rheingold, A.; Petrouleas, V.; Stubbe, J.; Armstrong, W. H.; Beer, R.; Lippard, S. J. *J. Am. Chem. Soc.* **1987**, *109*, 1435−1444.
(38) Wieghardt, K.; Bossek, U.; Nuber, B.; Weiss, J.; Bonviosin, J.; Corbella, M.; Vittols, S.; Gieed, J.-J. *J. Am. Chem. Soc.* **1988**, *110*, 7398−7405.
(39) Bordwell, F. G.; Zhang, X.-M.; Cheng, J.-P. *J. Org. Chem.* **1993**, *58*, 6410−6416.
(40) Baldwin, M.; Pecoraro, V. L. *J. Am. Chem. Soc.* **1995**, *118*, 11325−11326.
(41) Hoganson, G. W.; Lydakis-Symantiris, N.; Tang, X.-S.; Tommos, C.; Warncke, K.; Babcock, G. T.; Diner, B. A.; McCracken, J.; Styring, S. *Photosynth. Res.* **1995**, *46*, 177−184.
(42) Gilchrist, M. L.; Ball, J. A.; Randall, D. W.; Britt, D. *Proc. Natl. Acad. Sci. U.S.A.* **1995**, *92*, 9545−9549.
(43) Tang, X.-S.; Randall, D. W.; Force, D. A.; Diner, B. A.; Britt, R. D. *J. Am. Chem. Soc.* **1996**, *118*, 7638−7639.
(44) Wang, S.; Folting, K.; Streib, W. E.; Schmitt, E. A.; McCusker, J. K.; Hendrickson, D. N.; Christou, G. *Angew. Chem., Int. Ed. Engl.* **1991**, *30*, 305−306.
(45) Kerr, J. A.; *CRC Handbook of Chemisry and Physics*, 77th ed.; Cleveland, OH, 1996; pp 9−51.
(46) Lind, J.; Shen, X.; Eriksen, T. E.; Merenyi, G. J. *J. Am. Chem. Soc.* **1990**, *112*, 479−482.
(47) Christou, G. *Acc. Chem. Res.* **1989**, *22*, 328−335.
(48) Kulawiec, R. J.; Crabtree, R. H.; Brudvig, G. W.; Schulte, G. K. *Inorg. Chem.* **1988**, *27*, 1309−1311.
(49) Aromi, G.; Wemple, M. W.; Aubin, S. J.; Folting, K.; Hendrickson, D. N.; Christou, G. *J. Am. Chem. Soc.* **1998**, *120*, 5850−5851.
(50) Zheng, M., Khangulov, S. V.; Dismukes, G. C.; Barynin, V. V. *Inorg. Chem.* **1994**, *33*, 382−387.

Table 1. Enthalpies for Reactions of PzH, O_2, $Mn_4O_4(Ph_2PO_2)_6$ (**1**), and $Mn_4O_2(Ph_2PO_2)_6$ (**2**)

#	reaction	ΔH (kcal/mol)	ref
1	4 pzH → 4 pz• + 4 [H]	+329.2	39
2	4[H] + 2[O] → 2 H_2O	−442	45,46
3	**1** + 4 pzH → **2** + 4 pz• + 2 H_2O	<0(spontaneous)	
4 = 3 − 1 − 2	**1** → **2** + 2[O]	<−112.8	
5	2[O] → O_2	−119	45,46
6 = 4 + 5	**1** → **2** + O_2	<−231.8	

this thermodynamic cycle, an upper estimate of <−112.8 kcal/mol for the dissociation of two O atoms from **1** is obtained. Using eq 4, we can also predict an upper estimate of <−231.8 kcal/mol for the enthalpy change for formation of O_2 + **2** from **1**, eq 6, from the measured bond dissociation enthalpy for O_2, eq 5 (Table 1). Although this thermodynamic cycle predicts a substantial driving force for the spontaneous evolution of dioxygen from **1**, this reaction is not observed (in the ground state) at room temperature, suggesting that there is a large activation barrier that must be overcome in the ground-state electronic surface. Part of this kinetic barrier can be attributed to an anticipated Franck−Condon barrier against the structural rearrangement of **1** that is needed as precursor to O−O bond formation and O_2 release. The O−O′ distances in **1** (across the faces of the cube) are 2.53−2.60 Å, which indicate a very weak interaction (van der Waals radii for two O atoms are 2.8 Å) compared to the covalent bond length of 1.45 Å for H_2O_2.

The foregoing results suggest that the $Mn_4O_4^{6+}$ to $Mn_4O_2^{6+}$ core conversion, starting from **1**, can be initiated by reductive dehydrogenation in the ground state using an H-atom donor (pzH). The structure of the dehydrated core has not been established conclusively, but all available evidence is consistent with a deoxygenated cubane core like that given in Scheme 1, or possibly an open butterfly core with rapid averaging by ligand exchange. An open butterfly core structure is present in the stable complex, $Mn_4O_2(RCO_2)_6(bpy)_2$ containing Mn_4(2II, 2III), which is prepared using bridging carboxylate ligands, and also in the Mn_4(4III) complexes illustrated by $[Mn_4O_2(RCO_2)_7(pic)_2]^-$ (pic = picolinate).[47,48] These latter complexes were not found to bind O_2 or to form cubane cores upon oxidation and, thus far, have not been shown to be models of the WOC core. The pseudocubane complex, $Mn_4O_3(O_2CCD_3)_4(dbm)_3$ containing a Mn_4(3III,IV)O_3O' core, does undergo ligand displacement of the unique μ_3-carboxylate upon reaction with methoxide or hydroxide.[49] Thus, the $1e^-/1H^+$ reduced core, $[Mn_4O_3(OH)]^{6+}$, can be trapped using this mixed-ligand set (carboxylato and dbm^- ligands), unlike the present case, with all phosphinato ligands.

Conclusions

The reduction chemistry in Scheme 1 constitutes the first example of a net four-electron plus four-proton transfer process involving interconversion between stable Mn clusters. This chemistry leads to the release of two water molecules, a reaction formally analogous to the reverse sequence of steps that occur in the S_0 to S_4 transitions prior to photosynthetic O_2 evolution. The "cubane-butterfly" core conversion, **1** → **2** + O_2, is analogous to a model conjectured for a possible structural rearrangement that triggers O_2 release during the final step of photosynthetic water oxidation, $S_3 \rightarrow S_4^* \rightarrow S_0 + O_2$.[21] Our data show that O_2 release via this core conversion is strongly prohibited for cases in which all six faces of the cubane are encumbered by facially bridging phosphinate ligands.

Acknowledgment. This research was supported by the National Institutes of Health, Grant No. GM39932. We are grateful to István Pelczer for advice on the NMR experiments.

Abbreviations: ESIMS, electrospray ionization−mass spectrometry; LDI-TOF, laser desorption ionization−time of flight; pzH, phenothiazine; EPR, electron paramagnetic resonance; WOC, water oxidizing complex; PSII, photosystem II; ZFS, zero field splitting.

Supporting Information Available: Cyclic voltammogram of **1**, UV−vis spectra of pzH, pz• and $pzH^{\bullet+}$; NMR spectra of phenothiazine reduced solutions of **1**, IR spectra of **1**, its isolated reduced form after phenothiazine treatment and $[MnL_2(py)_2]$, EPR spectra of **2** with a plot of their temperature dependence, EPR titration of **1** with pzH, FTIR spectra of reaction mixtures of 1 and pzH, pzH and H_2O in CH_2Cl_2. This material is available free of charge via the Internet at http://pubs.acs.org.

IC9911421